

Photodissociation spectroscopy of Al + -acetaldehyde

W.-Y. Lu, M. Acar, and P. D. Kleiber

Citation: *The Journal of Chemical Physics* **116**, 4847 (2002); doi: 10.1063/1.1452729

View online: <http://dx.doi.org/10.1063/1.1452729>

View Table of Contents: <http://scitation.aip.org/content/aip/journal/jcp/116/12?ver=pdfcov>

Published by the [AIP Publishing](#)

Articles you may be interested in

[Photodissociation and photoionization of 2,5-dihydroxybenzoic acid at 193 and 355 nm](#)

J. Chem. Phys. **133**, 244309 (2010); 10.1063/1.3518709

[Photodissociation spectroscopy of Mg + -acetaldehyde](#)

J. Chem. Phys. **114**, 10288 (2001); 10.1063/1.1374579

[Ultraviolet/infrared-double resonance spectroscopy and ab initio calculations on the indole + and indole\(H₂O\)⁺ cations](#)

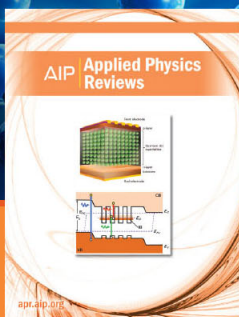
J. Chem. Phys. **113**, 7945 (2000); 10.1063/1.1315610

[Photodissociation spectroscopy of MgO₂ +](#)

J. Chem. Phys. **109**, 8311 (1998); 10.1063/1.477494

[Infrared photodissociation spectra of CH₃ + -Ar_n complexes \(n=1-8\)](#)

J. Chem. Phys. **108**, 10046 (1998); 10.1063/1.476465



NEW Special Topic Sections

NOW ONLINE
Lithium Niobate Properties and Applications:
Reviews of Emerging Trends

AIP | Applied Physics
Reviews

Photodissociation spectroscopy of Al^+ -acetaldehyde

W.-Y. Lu, M. Acar, and P. D. Kleiber

Department of Physics and Astronomy, and Optical Science and Technology Center, University of Iowa, Iowa City, Iowa 52242

(Received 5 November 2001; accepted 3 January 2002)

We have investigated the photodissociation spectroscopy of the Al^+ -acetaldehyde bimolecular complex over the spectral range 212–345 nm. We find evidence for three overlapping molecular absorption bands in the near UV. Two of the bands are unstructured and are assigned as $1A''$ and $2A'' \leftarrow 1A'$. These continuum bands are of mixed character with contributions from Al^+ -centered $3p\pi(A'') \leftarrow 3s\sigma(A')$, acetaldehyde-centered $\pi^*(A'') \leftarrow n(A')$, and Al -acetaldehyde charge transfer excitation processes. The third absorption band at short wavelengths, $\lambda > 223$ nm, shows a prominent vibrational progression with a mode frequency $\omega_e = 210 \pm 4 \text{ cm}^{-1}$. The structured band is assigned as $2A' \leftarrow 1A'$ and correlates to an Al^+ -centered $3p\pi(A') \leftarrow 3s\sigma(A')$ radiative transition; the vibrational progression is assigned to the intermolecular Al^+ -acetaldehyde *in-plane* bend. Spectroscopic results are in good agreement with *ab initio* predictions. © 2002 American Institute of Physics. [DOI: 10.1063/1.1452729]

I. INTRODUCTION

The interactions of metal ions with hydrocarbons are important in organometallic chemistry, biochemistry, and catalysis. Significant work has gone into investigating metal ion-hydrocarbon reaction mechanisms and energetics.^{1–9} In this effort, the photodissociation spectroscopy of weakly bound metal ion hydrocarbon complexes has proven to be a valuable tool, providing detailed information about intermolecular interactions and insight into the chemical dynamics.^{6–9}

We have used photodissociation spectroscopy to probe metal ion-hydrocarbon interactions in a series of weakly bound complexes of light metal ions with small alkanes and alkenes.^{9–17} Recently, we extended this method to investigate the more strongly bound Mg^+ -acetaldehyde complex.^{18,19} Mg^+ binds to the O-atom in end-on $\text{Mg}^+-\text{O}-\text{C}$ geometry because the binding is primarily electrostatic in nature and oxygen has a high electronegativity. The Mg ion-carbonyl intermolecular bond is stronger than a typical metal ion-rare gas or metal ion-hydrocarbon bond. *Ab initio* calculations show that the strong electrostatic bond results in part from a polarization of the oxygen charge toward the metal cation, which in turn causes a slight weakening and stretching of the carbonyl O–C bond.²⁰ Photodissociation spectroscopy allows us to probe metal-carbonyl bimolecular interactions under isolated gas-phase conditions and offers a useful test of *ab initio* model predictions. In addition, photodissociation of the weakly bound complex mimics a bimolecular “half-collision” and offers unique insight into metal-carbonyl reaction dynamics.¹⁹

In Mg^+ -acetaldehyde we found four distinct absorption bands correlating to Mg^+ -centered ($3p \leftarrow 3s$) and acetaldehyde-centered ($\pi^* \leftarrow n$) radiative transitions in the complex.¹⁸ Our results showed that the Mg^+ -centered $3p\pi(A'') \leftarrow 3s\sigma(A')$ and acetaldehyde-centered $\pi^*(A'') \leftarrow n(A')$ transitions are mixed, resulting in substantial vibra-

tional excitation in the complex and leading to broad unresolved absorption bands. In contrast, the predominantly Mg^+ -centered excitation bands, assigned as $3p\pi(A'') \leftarrow 3s\sigma(A')$ and $3p\sigma(A') \leftarrow 3s\sigma(A')$ each show prominent vibrational structure. Nonreactive dissociation to the bare metal ion, Mg^+ , is the dominant photolysis channel throughout the near UV. However, excitation in the $3p\sigma(A') \leftarrow 3s\sigma(A')$ band, also results in reactive quenching to MgH^+ , MgCHO^+ , and MgCH_3^+ products. Our results suggest that the reaction may occur in a single step process through direct metal ion attack on the aldehydic C–H or C–C bonds.¹⁹ The reasons for the σ -like orbital alignment preference for reaction are not fully understood although simple energetics may play a role: excitation to $\text{Mg}^+(3p\sigma(A'))$ occurs at higher energies, possibly above a reaction barrier in the excited state.

Here we report on the photodissociation spectroscopy of Al^+ -acetaldehyde in the near UV. This work offers an interesting comparison with our previous studies of Mg^+ -acetaldehyde. The difference in metal ion electronic valence may have an appreciable effect on the binding and structure of the complex. The $\text{Al}^+ 3s3p \leftarrow 3s^2$ resonance line lies at much higher energy raising the possibility that additional reaction channels may be open. Indeed, in a recent study of the collision-induced dissociation of Al^+ -acetaldehyde clusters, a complicated reaction product mass spectrum was observed showing major peaks for H-atom and H_2 -molecule loss, and a host of minor product peaks including AlO^+ , AlCO^+ , AlOH^+ , and AlCOH^+ .²¹ Photodissociation of isolated $\text{Al}^+(\text{CH}_3\text{CHO})$ bimolecular complexes could allow us to probe such chemical processes under more carefully controlled “half-collision” conditions.

II. ELECTRONIC STRUCTURE CALCULATIONS

Ab initio calculations on the GAUSSIAN 94 platform show Al^+ -acetaldehyde to be moderately strongly bound by elec-

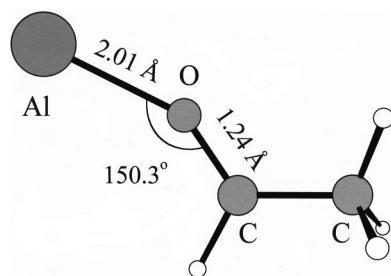


FIG. 1. The ground-state geometry of $\text{Al}^+-\text{CHOCH}_3$ calculated at MP2/6-311++g(2d,2p) level.

trostatic forces in an equilibrium $\text{Al}^+-\text{OCHCH}_3$ C_s -structure (Fig. 1). The equilibrium Al–O bond length is $R_{\text{Al-O}}=2.01$ Å with an M–O–C bond angle of 150° at the MP2/6-311++g(2d,2p) level. The acetaldehyde moiety is relatively undistorted with a planar OCCH structure and a slightly elongated C=O bond. ($R_{\text{CO}}=1.24$ Å in the complex, which may be compared with the value of 1.19 Å in isolated acetaldehyde.) The Al–O bond dissociation energy (without zero-point energy or basis set superposition error corrections) is $D_e''(\text{Al-O})=1.47$ eV at the QCISD(T)//MP2/6-311++g(2d,2p) level. This may be compared with the earlier value of 1.57 eV (after zero-point energy correction) of Tortajada.²¹ The $\text{Al}^+-\text{CH}_3\text{CHO}$ equilibrium structure and binding energy are very similar to that found previously for $\text{Mg}^+-\text{CH}_3\text{CHO}$, with only a slightly weaker and longer M–O bond in the Al^+ case: $R_{\text{Mg-O}}=1.96$ Å and $D_e''(\text{Mg-O})=1.55$ eV.¹⁸ The change in metal ion valence to a closed $3s^2$ shell appears to have a relatively small effect on the binding in the complex which is predominantly electrostatic. The major difference in structure is in the M–O–C bond angle with the Al-complex bent toward the aldehydic H-atom in a sharper angle (150° versus 172° in the Mg^+ case). However, the potential is relatively flat in this bending angle and we expect that the complex will be floppy with large zero-point motions in the ground state for the *in-plane* bend. We have also carried out a calculation of the SCF vibrational frequencies in the ground state. The intermolecular vibrational mode frequencies are calculated as 290 cm^{-1} for the intermolecular Al–O stretch, and 69 (165) cm^{-1} for the *in-plane* (*out-of-plane*) intermolecular bending motions, respectively.

The excited state structure is complicated, with a large number of active orbitals and interacting electronic states. Radiative transitions to low-lying excited states with metal-centered $p\leftarrow s$, aldehyde-centered $\pi^*\leftarrow n$, and aldehyde-metal charge-transfer character may all be possible. To help clarify the spectral assignment we have carried out a configuration interaction with single excitations calculation [CIS/6-311++g(2d,2p)] for the low-lying excited states. The CIS method works well for radiative transitions that can be well characterized as Al^+ -centered $3s3p\leftarrow 3s^2$ excitations. For example, the calculated Al^+ excited state resonance energy is accurate to better than 0.1 eV at the CIS level (7.46 eV calculated versus 7.42 eV experimental). However, the CIS method is much less reliable for the acetaldehyde-centered or charge transfer excitation processes

TABLE I. HF/CIS optimized geometries for the ground ($1A'$) and excited ($1A''$, $2A'$) states.

State	R(Al–O) (Å)	R(C–O) (Å)	Angle (Al–O–C)
($1A'$)	1.94	1.219	158°
($1A''$)	1.60	1.326	165°
($2A'$)	1.82	1.233	136°

that involve a change in bond order or where correlation effects are likely to be more important. The theoretical energies for both the acetaldehyde excited state and the charge transfer asymptote are in error by more than 1 eV. MCSCF calculations are difficult owing to the lack of symmetry, and the large number of active orbitals and interacting excited states, leading to convergence problems. As a result we must rely largely on qualitative considerations to assign the observed spectrum.

CIS calculations find three low-lying excited states, $1A''$, $2A'$, and $2A''$, with vertical excitation energies of 5.54 eV ($\lambda=224$ nm), 6.05 eV ($\lambda=205$ nm), and 6.05 eV ($\lambda=205$ nm), respectively. NBO molecular orbital occupation analysis shows that the $2A'\leftarrow 1A'$ transition is well characterized as an Al^+ -based $3p\pi(A')\leftarrow 3s\sigma(A')$ process; we may then expect that the corresponding prediction of a strong absorption band centered near 205 nm should be good for this metal-centered transition. In contrast both the $1A''$ and $2A''\leftarrow 1A'$ transitions are of mixed character with contributions from Al^+ -based $3p\pi(A'')\leftarrow 3s\sigma(A')$, acetaldehyde-based $\pi^*\leftarrow n$, and Al-acetaldehyde charge transfer processes. As a result we do not expect the vertical excitation energies for transitions to the A'' states to be especially accurate. We encountered a similar situation in previous work on Mg^+ -acetaldehyde and we may use the results from that study to help guide the spectral assignment here.¹⁸

We have also optimized the excited state geometries for both $1A''$ and $2A'$ at the CIS level and the results give useful insight into the excited state molecular orbital interactions. A comparison of the ground and excited state equilibrium geometries at the is given in Table I. Note that $1A''$ shows stronger chemical binding than either the ground ($1A'$) or excited ($2A'$) states, with a much shorter Al–O bond and longer C–O bond. This result can be understood in terms of the molecular orbital interactions. The transition carries a substantial acetaldehyde-centered $\pi^*\leftarrow n$ character. This process corresponds to excitation from a nonbonding orbital centered on the O atom to the π^* antibonding LUMO of acetaldehyde centered on the C–O bond. This excitation weakens the C–O bond. In addition, in this orbital symmetry there is the possibility for transferring electron density from the π^* orbital of C–O to the empty Al^+ *out-of-plane* p -orbital that leads to formation of a partial Al–O chemical bond. $1A''\leftarrow 1A'$ excitation will be accompanied by a significant bonding and geometry change with rapid IVR, and is likely to result in a dense and unresolved absorption spectrum.

In contrast the Al^+ -based $2A'\leftarrow 1A'$ transition corresponds to exciting the Al^+ *in-plane* p -orbital that is roughly perpendicular to the Al–O bond. In this symmetry the mo-

molecular orbital interactions are expected to be weaker and $2A'$ shows a much less pronounced geometry change on Franck–Condon excitation from the ground state. We may then expect a relatively simpler vibrational spectrum in $2A'$ featuring prominent low-frequency intermolecular vibrational motions. For comparison with experimental spectroscopic data below we have calculated the vibrational mode frequencies in $2A'$. The intermolecular vibrational modes have frequencies of 422 cm^{-1} for the intermolecular stretch, and 207 (157) cm^{-1} for the *in-plane* (*out-of-plane*) bending motions, respectively.

III. EXPERIMENTAL ARRANGEMENT

The experimental apparatus used for mass-selected photodissociation spectroscopy has been described previously.⁹ Al^+ - CH_3CHO complexes are produced in a supersonic molecular beam expansion with a laser vaporization source. A 2% mixture of acetaldehyde in Ar was used at a backing pressure of 60 psi. The second harmonic (532 nm) of a Nd:YAG laser was weakly focused onto a rotating Al rod and timed to overlap the gas pulse. Downstream from the molecular beam skimmer, ion clusters are extracted and accelerated into the flight tube of an angular reflection time-of-flight mass spectrometer. The source mass spectrum is clean, showing strong peaks that correspond to the family of cluster ions $\text{Al}(\text{CH}_3\text{CHO})_n^+$. The bimolecular parent complex, $\text{Al}(\text{CH}_3\text{CHO})^+$, was mass-selected by a pulsed electric field to deflect unwanted ions from the source. At the turning point inside the reflection, a frequency doubled Nd:YAG laser pumped tunable OPO (Spectra-Physics/Quanta-Ray PRO-250/MOPO-SL) was time-delayed to excite the parent $\text{Al}(\text{CH}_3\text{CHO})^+$ ion. Parent and daughter ions were then re-accelerated to an off-axis MCP detector and mass analyzed in a standard tandem time-of-flight arrangement. Digital oscilloscopes, a multichannel scaler, and a set of gated integrators are used to monitor the mass spectrum, and are interfaced to a computer to record the data for further analysis. The Al^+ action spectrum is determined by normalizing the daughter signal with respect to the parent signal and laser power while scanning the photon wavelength. A laser power dependence test indicated that the absorption is a one-photon process.

IV. RESULTS AND DISCUSSION

The photodissociation action spectrum for Al^+ -acetaldehyde over the range 212–345 nm is shown in Fig. 2. Three absorption features are observed. There is a very weak continuum band in the range 265–345 nm, centered near 285 nm. Starting from 265 nm and rising toward higher energy there is a much stronger continuum absorption feature. At still higher energies ($\lambda < 223$ nm) we see the onset of a long harmonic vibrational progression that overlies the continuum band. Al^+ is the only fragment observed through the absorption spectrum.

A. $1A'' \leftarrow 1A'$ band

The lowest energy band centered near 285 nm is assigned as $1A'' \leftarrow 1A'$. The band position and breadth are

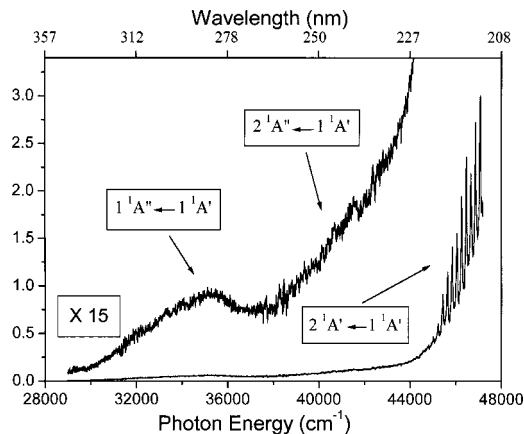


FIG. 2. Photodissociation spectrum of Al^+ - CHOCH_3 in the 212–345 nm range.

very similar to the $S_1 \leftarrow S_0$ ($\pi^* \leftarrow n$) absorption band of bare CH_3CHO observed under low resolution.²² We also observed a similar band in our previous work on Mg^+ -acetaldehyde.¹⁸ Based on these similarities we assign the weak low-energy continuum band centered at 285 nm to an acetaldehyde-based $\pi^*(1A'') \leftarrow n(1A')$ transition. The observed band position at 285 nm is in relatively poor agreement with the CIS prediction of 224 nm. As noted this is not surprising since the asymptotic acetaldehyde $\pi^* \leftarrow n$ transition is also in error in the CIS calculation by ~ 1 eV. If we correct this asymptotic energy shift the agreement becomes quite reasonable (~ 285 nm observed versus ~ 275 nm estimated) giving further support to the assignment.

As suggested by the *ab initio* results, we expect that this orbital characterization is not entirely rigorous and that the band involves some admixture of acetaldehyde-based, Al^+ -based, and Al-acetaldehyde charge transfer excitation character. This coupling can lead to a shift and enhancement of the nominally weak acetaldehyde-based absorption band. However, the strong similarities between the Al^+ -acetaldehyde, Mg^+ -acetaldehyde, and bare acetaldehyde absorption features in this range suggest that the mixing may not be extensive and this orbital characterization pedagogically useful.

The $\pi^* \leftarrow n$ transition in bare acetaldehyde is known to lead to a complicated and dense vibrational spectrum that is not completely assigned, but includes substantial excitation of the methyl torsion, C–H wag, CCO deformation, and CO stretch modes.²² The lack of observed structure in the $1A'' \leftarrow 1A'$ continuum band of Al^+ -acetaldehyde probably results from fast IVR and a complicated and unresolved vibrational spectrum in a distorted excited state complex. This result is also consistent with the large bonding and geometry change expected from the *ab initio* calculations as discussed. Dissociation probably occurs through coupling to ground-state surface although direct coupling to the ground state is forbidden by symmetry so distortion of the complex out of C_s symmetry is required.

B. $2A'' \leftarrow 1A'$ band

Starting from about 265 nm a stronger continuum band rises to the short wavelength limit of our laser system at 212

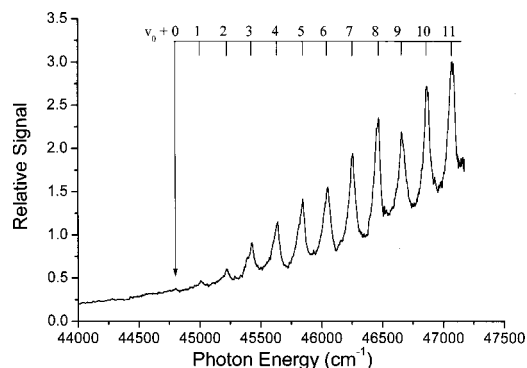


FIG. 3. Expanded view of the $2^1A' \leftarrow 1^1A'$ band showing the vibrational structure.

nm. Like the lower-energy band, this band is probably somewhat mixed. However, its relative strength suggests it has appreciable metal-centered excitation character. The band is assigned as $2A'' \leftarrow 1A'$ and correlates to a predominantly Al^+ -centered $3s\sigma 3p\pi \leftarrow 3s^2$ transition with the Al p -orbital lying perpendicular to the molecular symmetry plane. The band position is consistent with the CIS calculated vertical excitation wavelength for $2A'$ of 205 nm.

The lack of any resolvable vibrational structure probably again results from fast IVR in the excited-state complex. In this symmetry Al^+ $3p$ orbital can overlap the acetaldehyde π^* -LUMO, allowing for the efficient transfer of electron density into the carbonyl antibonding orbital. This process corresponds to the “half-collision” analog to $E-E$ energy transfer quenching. (Equivalently, in the bimolecular complex, the metal-centered $3s3p \leftarrow 3s^2$ transition can mix with the nearby acetaldehyde-based $\pi^* \leftarrow n$ transition of the same symmetry as discussed.) This leads to a weakening of the CO bond and appreciable distortion of the complex in the excited state.

C. $2A' \leftarrow 1A'$ band

Starting from 223 nm, we observe the onset of a prominent vibrational progression indicating a strong new absorption band that overlaps the continuum $2A'' \leftarrow 1A'$ band. This structured band is assigned as $2A' \leftarrow 1A'$, correlating to the Al^+ -based $3s\sigma 3p\pi \leftarrow 3s^2$ transition with the Al p -orbital lying in the symmetry plane but roughly perpendicular to the $Al^+ - O$ bond. The CIS predicted position for this band is 205 nm.

A detailed view of the vibrational resonance structure is depicted in Fig. 3 and the corresponding peak positions and assignments are given in Table II. The obvious vibrational progression shows a mode spacing of ~ 210 cm^{-1} . Because the Franck-Condon envelope is falling toward the red end of the spectrum, we cannot definitively assign the band origin. However, because the progression is long and harmonic we suspect these vibrational levels are probably low in the excited-state potential well and that the first observed resonance is close to the band origin. Further evidence to support this suggestion can be gleaned from isotope substitution experiments discussed below. Assuming the first observed resonance at $44\,800$ cm^{-1} to be the origin, Birge-Sponer analy-

TABLE II. Vibration peak position and assignment in the $2^1A' \leftarrow 1^1A'$ transition.

Peak position (cm^{-1}) ^{a,b}	Assignment ($v_0 + n$) ^c
44 800 (?)	0
45 005 (45 015)	1
45 219 (45 221)	2
45 424 (45 410)	3
45 636 (45 592)	4
45 843 (45 777)	5
46 049 (45 972)	6
46 253 (46 164)	7
46 466 (46 337)	8
46 655 (46 529)	9
46 862 (46 717)	10
47 068 (46 904)	11
(?) (47 086)	12

^aPeak positions for the isotopomer $Al^+(CD_3CDO)$ are given in parentheses.

^bUncertainty in the peak position is typically ± 8 cm^{-1} owing to the large resonance widths.

^cThe vibrational mode is assigned as the a' *in-plane* intermolecular bend. The absolute vibrational numbering is uncertain but v_0 is probably close to 0.

sis gives a fundamental vibrational frequency as $\omega'_e = 210 \pm 4$ cm^{-1} with an anharmonicity parameter of $\omega_e x'_e = 0.32 \pm 0.31$ cm^{-1} . (Because of the relatively small anharmonicity, the assumed vibrational numbering probably does not introduce a significant additional error in the fundamental frequency.)

This vibrational mode is probably not associated with any of the intramolecular acetaldehyde vibrations. All of these (except the CH_3 torsion) are significantly higher in energy. The CH_3 torsional mode frequency is comparable (~ 100 – 150 cm^{-1}) but it has a barrier to free rotation of < 1000 cm^{-1} .²² Since the progression here is harmonic over an energy range > 2000 cm^{-1} , it cannot be the methyl torsion. This mode progression must be associated with one of the three intermolecular vibrational modes of the Al -acetaldehyde complex.

There are relatively few studies of the intermolecular vibrations in Al^+ -molecule complexes. The most likely candidates for the observed mode are the intermolecular $Al-O$ stretch and the $Al-O-C$ *in-plane* bend, both a' . Based on our experience with other weakly bound metal ion-molecule complexes, a long harmonic low-frequency progression typically points to an intermolecular stretch motion. However, the intermolecular frequency of $\omega_e = 210$ cm^{-1} observed here would be surprisingly low in comparison with the other bimolecular complexes that support a metal ion-oxygen intermolecular bond such as $Mg^+ - H_2O$, $Mg^+ - CH_3OH$, and $Mg^+ - CH_3CHO$. In these complexes the intermolecular stretch frequencies are 505, ~ 550 , and 384 cm^{-1} , respectively.^{6,18,23} It is not obvious why the stretch frequency in $Al^+ - CH_3CHO$ would be so much smaller. The observed frequency is also much lower than the SCF *ab initio* value for the $2A'$ state stretch of 422 cm^{-1} . The observed mode frequency is, however, very close to the SCF predicted frequency of 207 cm^{-1} for the *in-plane* intermolecular bend.

To clarify the vibrational assignment, we repeated the experiment with the isotopomer $Al^+(CD_3CDO)$. The ob-

served vibrational resonances are also given in Table II. The mode shows a substantial isotope shift with a fundamental frequency of $195 \pm 5 \text{ cm}^{-1}$ (and anharmonicity parameter $\omega_e x'_e = 0.44 \pm 0.31$). This isotope shift is larger than expected for the intermolecular stretch in a pseudodiatom approximation, but is in good agreement with the expected isotope shift for the *in-plane* bend. The SCF calculated frequency for the *in-plane* intermolecular bend in Al⁺(CD₃CDO) is 194 cm^{-1} . Based on this comparison we assign the observed vibrational mode to the *a'* intermolecular *in-plane* bend. The excellent agreement between the observed and SCF predicted vibrational frequencies support the calculated structure.

Note that the isotope shift in the first few observed resonance peaks is comparable to the experimental uncertainty and smaller than the widths of the observed resonances. This again suggests that the first observed resonance peak at $44\,800 \text{ cm}^{-1}$ is close to the origin of the excited-state potential. [The isotope shift in the origin band could be substantial for this H–D substitution, but it is probably not larger than the width of the observed vibrational resonance features ($\sim 50 \text{ cm}^{-1}$). For comparison the CD₃CDO–CH₃CHO zero-point shift in the $1^1A'' \leftarrow 1^1A' 0_0^0$ band of bare acetaldehyde is 37 cm^{-1} .²²]

V. COMPARISON WITH PREVIOUS WORK

A comparison with results from our previous spectroscopic work on Mg⁺–CH₃CHO is interesting.¹⁸ The binding energy and equilibrium intermolecular bond length is similar for each complex. In each case we find evidence for UV absorption bands that correlate with metal-based ($3p \leftarrow 3s$) and acetaldehyde-based ($\pi^* \leftarrow n$) transitions. Two of the bands, assigned as ($1A''$ and $2A'' \leftarrow 1A'$) appear as unstructured continuum bands. Our results suggest that these bands are of mixed metal-centered $3p\pi(A'') \leftarrow 3s\sigma(A')$ and acetaldehyde-centered $\pi^*(A'') \leftarrow n(A')$ character. In each case the *A''* excited-state complex is expected to be appreciably distorted, resulting in fast IVR and complex and unresolved vibrational structure in these absorption bands. In contrast, the $2A' \leftarrow 1A'$ band that correlates with the metal-based $3p\pi(A') \leftarrow 3s\sigma(A')$ transition, shows prominent vibrational resonance structure in each complex that can be assigned to the intermolecular *in-plane* bend. In Mg⁺(CH₃CHO) the *in-plane* vibrational progression was short and anharmonic with an apparent isomerization barrier of $\sim 900 \text{ cm}^{-1}$. In Al⁺(CH₃CHO) the corresponding progression is long and harmonic, suggesting that internal rearrangement is more difficult.

Absorption in the blueshifted $3p\sigma(A') \leftarrow 3s\sigma(A')$ band of Mg⁺-acetaldehyde yields a weak but clear branching to chemical quenching products MgH⁺, MgCH₃⁺, and MgCHO⁺ that involve C–H and C–C bond cleavage. Experimental results suggest that reaction involves direct insertion of the metal ion into aldehydic C–H or C–C bonds, with roughly comparable yields.¹⁹ In the $3p\sigma$ excited state the Mg⁺ valence *p*-orbital lies roughly along the Mg⁺–O–C bond. No reaction was observed following excitation in the $3p\pi \leftarrow 3s\sigma$ bands. The reasons for this electronic orbital

alignment preference for reaction are not obvious but we suggested that simple energetics might play a role. The $3p\sigma \leftarrow 3s\sigma$ band lies at higher energy and may simply be above an energetic threshold for reaction.

Because of the high Al⁺ $3s \leftarrow 3p$ resonance energy, the metal-centered $3p\pi \leftarrow 3s\sigma$ bands lies at fairly high energy and we had anticipated that reactive dissociation products might be observed. However, we see no evidence for any reaction product in these bands, suggesting that the origin of the observed orbital alignment preference for reaction in Mg⁺-acetaldehyde may be dynamical and not simply energetic. In this regard note that the initial M⁺ *pσ*-orbital alignment is with respect to the M–O bond. However, in an *in-plane* intermolecular bend this M⁺ *p*-orbital alignment becomes π -like with respect to the aldehydic C–H or C–C bonds. In this symmetry a bond stretch insertion process facilitated by overlap with the localized σ^* -antibonding orbitals centered on the C–H or C–C bonds might be possible.⁹ Based on this we expect that Al⁺($3s\sigma 3p\sigma$) should react similarly with acetaldehyde although this state lies at higher energy, beyond the limit of our laser system.

It is also worth noting that Tortajada *et al.* have investigated Al⁺-acetaldehyde using collision-induced-dissociation (CID) methods.²¹ Upon collisional activation, several reaction products were observed with major channels corresponding to H- and H₂-loss and a number of minor reaction channels yielding AlO⁺, AlCO⁺, AlOH⁺, AlCOH⁺ products. In contrast we observe only the nonreactive quenching to the Al⁺ daughter ion in our photodissociation study. Of course the CID experiments involve higher energy, and reactions are likely to proceed through multiple steps with complicated rearrangement and fragmentation. In contrast, the photodissociation method is relatively “soft” and involves a single-step process in a controlled O-end on approach geometry. In both Mg⁺- and Al⁺-CH₃CHO it appears that reactive quenching of the excited *p*-state metal ion is inefficient for O-end on approach in π -orbital alignment. Rather the dominant quenching mechanism for this approach geometry is through inelastic *E-E* and *E-V* energy-transfer quenching.

ACKNOWLEDGMENTS

This research has been carried out with support from the National Science Foundation and from the Donors to the Petroleum Research Fund of the American Chemical Society.

¹K. Eller and H. Schwarz, Chem. Rev. **91**, 1121 (1991).

²P. B. Armentrout, Acc. Chem. Res. **28**, 430 (1995); in *Selective Hydrocarbon Activation: Principles and Progress*, edited by J. A. Davies, P. L. Watson, J. F. Liebman, and A. Greenberg (VCH, New York, 1990).

³J. C. Weisshaar, Acc. Chem. Res. **26**, 213 (1993); Adv. Chem. Phys. **82**, 213 (1992).

⁴P. A. M. Van Koppen, R. R. Kemper, and M. T. Bowers, in *Organometallic Ion Chemistry*, edited by B. S. Freiser (Kluwer Academic, Boston, MA, 1996).

⁵B. S. Freiser, Acc. Chem. Res. **27**, 353 (1994); J. Mass Spectrom. **31**, 703 (1996).

⁶J. S. Pilgrim, C. S. Yeh, K. F. Willey, D. L. Robbins, and M. A. Duncan, Int. Rev. Phys. Chem. **13**, 231 (1994); M. A. Duncan, Annu. Rev. Phys. Chem. **48**, 69 (1997).

⁷J. M. Farrar, in *Cluster Ions*, edited by C. Y. Ng, T. Baer, and I. Powis (Wiley, New York, 1993), p. 243.

- ⁸D. E. Lessen, R. L. Asher, and P. J. Brucat, in *Advances in Metal and Semiconductor Clusters*, Vol. I, edited by M. A. Duncan (JAI, Greenwich, CT, 1983), p. 267; *Int. J. Mass Spectrom. Ion Processes* **102**, 331 (1990).
- ⁹P. D. Kleiber and J. Chen, *Int. Rev. Phys. Chem.* **17**, 1 (1998).
- ¹⁰L. N. Ding, M. A. Young, P. D. Kleiber, W. C. Stwalley, and A. M. Lyyra, *J. Phys. Chem.* **97**, 2181 (1993).
- ¹¹Y. C. Cheng, J. Chen, L. Ding, T. H. Wong, P. D. Kleiber, and D. K. Liu, *J. Chem. Phys.* **104**, 6452 (1996).
- ¹²J. Chen, Y. C. Cheng, and P. D. Kleiber, *J. Chem. Phys.* **106**, 3884 (1997).
- ¹³W.-Y. Lu, T.-H. Wong, and P. D. Kleiber, *Chem. Phys. Lett.* **347**, 183 (2001).
- ¹⁴J. Chen, T. H. Wong, K. Montgomery, Y. C. Cheng, and P. D. Kleiber, *J. Chem. Phys.* **108**, 2285 (1998).
- ¹⁵J. H. Holmes, P. D. Kleiber, D. A. Olsgaard, and K. H. Yang, *J. Chem. Phys.* **112**, 6583 (2000).
- ¹⁶J. Chen, T. H. Wong, P. D. Kleiber, and K. H. Yang, *J. Chem. Phys.* **110**, 11798 (1999).
- ¹⁷W.-Y. Lu, P. D. Kleiber, M. A. Young, and K.-H. Yang, *J. Chem. Phys.* **115**, 5823 (2001).
- ¹⁸W.-Y. Lu and P. D. Kleiber, *J. Chem. Phys.* **114**, 10288 (2001).
- ¹⁹W.-Y. Lu and P. D. Kleiber, *Chem. Phys. Lett.* **338**, 291 (2001).
- ²⁰H. Partridge and C. W. Bauschlicher, Jr., *J. Phys. Chem.* **96**, 8827 (1992).
- ²¹J. Tortajada, A. Total, J. P. Morizur, M. Alcamí, O. Mo, and M. Yanez, *J. Phys. Chem.* **96**, 8309 (1992).
- ²²M. Noble and E. K. C. Lee, *J. Chem. Phys.* **81**, 1632 (1984).
- ²³M. R. France, S. H. Pullins, and M. A. Duncan, *Chem. Phys.* **239**, 447 (1998).